PHYSICAL REVIEW B VOLUME 18, NUMBER 2 15 JULY 1978

Theory of electron-hole liquid in semiconductors

G. Beni
Bell Laboratories, Holmdel, New Jersey 07733

T. M. Rice
Bell Laboratories, Murray Hill, New Jersey 07974

(Received 19 January 1978)

The random-phase approximation is generalized to include the effects of band anisotropy, coupling between degenerate valence bands, coupling to optical phonons, and the Hubbard exchange correction. This method is used to calculate the ground-state energy and equilibrium density of the electron-hole liquid in Ge, Si, AgBr, and various II-VI and III-V compounds and the thallous halides and lead chalcogenides. The results are compared to the experiments where they are available. Agreement is excellent for Ge and Si and reasonable for the other materials, considering the large uncertainties in the values of the band masses, etc. Substantial discrepancies remain between theory and experiment, however, in the cases of GaAs and ZnO.

I. INTRODUCTION

Recently, it has become clear that electron-hole (*e*-*h*) liquid phases can be observed in a wide variety of semiconductors.[1] Following the early work on Ge and Si, compounds—where polar effects are important—have been studied. The *e*-*h* liquid has been observed recently in the indirect-gap materials GaP (Ref. 2) and AgBr (Ref. 3). It has also been found that in certain polar *direct*-gap semiconductors, such as CdS and CdSe,[4] the many-body interactions between carriers lower the band gap and lead to a stabilization of the *e*-*h* liquid phase. Such phases, in direct-gap semiconductors, exhibit stimulated emission and the theory of the energetics of these phases is important for the understanding of laser action.

At the same time, a theory of the *e*-*h* liquid in polar semiconductors has begun to develop.[5-7] In this paper, we present a detailed theory of the *e*-*h* liquid in these systems. We apply it to calculate the ground-state energy and the equilibrium densities of the *e*-*h* liquid in a large number of materials.

The development of the theory of the *e*-*h* liquid in polar semiconductors began with the observation by Keldysh and Silin[5] that the polar interaction should tend to stabilize the liquid phase. Their paper contains an analysis of the electron and hole exchange energies but no detailed discussion of the correlation energy. They found that the exchange energy is lowered by the polar interaction both in the high-density and in the low-density limits. Keldysh and Silin argued in favor of a lowering of the ground-state energy at any density.

This conclusion was reinforced by our work[6]—hereinafter referred to as I—in which we calculated the ground state energy of the *e*-*h* liquid for four polar semiconductors including the coupling to the LO phonons. We found that in CdS, CdSe, ZnS, and AgBr, the electron-phonon interaction increases the stability of the liquid phase relative to the excitons. In our approach we generalized the random-phase approximation (RPA) by adding the polarizability of the polar lattice to that of the carriers. The RPA is the basis for the successful theory of *e*-*h* liquid in the elemental semiconductors Ge and Si. It can be used for the densities of interest where high-density expansions break down.

To simplify the additional complications created by the inclusion of the phonon interaction, the ground-state energy was calculated in I using the plasmon-pole approximation[8] which is a simplified version of the RPA. (Rösler and Zimmerman[7] also used this approximation—albeit in a somewhat improved form—to calculate the phase diagram for *e*-*h* liquid formation.) The main advantages of the plasmon-pole approximation are its mathematical simplicity and its clear physical meaning. These advantages, however, are counter-balanced by a certain degree of arbitrariness in the choice of the parameters which leads to difficulty in applying the theory to semiconductors with a complex band structure. More precisely, the choice of the b coefficient in the plasmon energy dispersion $[\omega_q^2=\omega_p^2+aq^2+bq^4$ (see I)] is basically an uncontrolled approximation. The valence band structure of the semiconductors considered in I was simple and the results were not too sensitive to this parameter. The relationship of the plasma pole to the RPA has been explored recently by Rösler and

Zimmerman[7] (RZ) for CdS. They used this comparison to adjust the b coefficient and then applied their method to several other II-VI compounds. We have found that the electron (and hole) self-energy—and thus the e-h liquid ground state energy—is sensitive to the choice of b for semiconductors with the zinc-blende crystal structure which have a coupled valence-band structure. In addition, difficulties remain in treating the band anisotropies. In fact, it turns out that the plasmon pole approximation leads to errors of the order of $\approx 25\%$ in the case of the ground-state energy of the e-h liquid in GaP.[9]

In this paper, we will use the full RPA to describe the carrier polarizability and include the effects of band anisotropy and coupling between degenerate valence bands where it is appropriate. The Hubbard exchange correction is also included. The carrier polarizability is added to that of the lattice to obtain the total polarizability for the RPA. In the low-density limit this calculation reduces to that of weakly interacting polarons. In this limit then the main contribution is the single polaron energy shift. This shift is well known[10] for nondegenerate bands and it has been recently discussed for the case of coupled valence bands.[11,12] As the density is increased the importance of the Coulomb interaction grows relative to the lattice interaction until in the high-density limit, lattice effects are negligible. The theory is outlined in Sec. II.

In Sec. III we present results for a variety of semiconductors and compare to experiment where we can. We discuss first those with the wurtzite structure which have simple ellipsoidal electron and hole bands: CdS, CdSe, ZnO, ZnS. We also include the case of AgBr. The comparison is made to the results in the plasmon pole approximation that we have obtained previously for these materials. All these semiconductors have substantial polar coupling. Next we consider semiconductors in which the valence bands are coupled. We present new calculations for the elemental semiconductors Ge and Si, which treat the band structure more accurately. The cubic II-VI and III-V are also in this class and have polar coupling which varies from weak to fairly substantial values. Lastly, we consider a group of highly polar semiconductors characterized by orbitally degenerate holes: TlCl, TlBr, PbS, PbSe, PbTe.

Section IV is devoted to a summary and evaluation of the results. We find that for those compounds in which the plasma frequency ω_p is much smaller than the phonon frequency ω_L the full RPA may not be reliable. We argue that replacing the dynamic phonon by its static limit, i.e., screening the Coulomb interaction by the static dielectric constant ϵ_0, is a better approximation in this limit.

II. THEORY

As in the nonpolar case,[1] we use the effective mass approximation to describe the electrons and the holes near the band extrema. Thus the Hamiltonian of the system contains a kinetic energy term with effective masses determined by the band structure and Coulomb interactions reduced by the high-frequency dielectric constant.

The Hartree-Fock energy (per e-h pair) can be obtained exactly.[13,14] For a system of ν_e conduction bands and ν_h uncoupled valence bands we have

$$E_{\mathrm{HF}} = E_K + E_{\mathrm{ex}}, \tag{1}$$

$$E_K = \frac{2.2099}{r_s^2}\left(\frac{\mu}{\nu_e^{2/3} m_{de}} + \frac{\mu}{\nu_h^{2/3} m_{dh}}\right) E_R, \tag{2}$$

$$E_{\mathrm{ex}} = -\frac{0.9163}{r_s}\left[\nu_e^{-1/3}\phi(\rho_e) + \nu_h^{-1/3}\phi(\rho_h)\right] E_R, \tag{3}$$

where we have adopted the reduced units used in the e-h liquid literature. Wave vectors are measured in units of the effective Fermi wave vector

$$k_F = (3\pi^2 n)^{1/3}, \tag{4}$$

where n is the e-h pair density. Energies are measured in units of the effective Rydberg E_R ($\hbar = 1$),

$$E_R = \mu e^4/2\epsilon_\infty^2 = e^2/2\epsilon_\infty a_x \tag{5}$$

(ϵ_∞ is the high-frequency dielectric constant; a_x is the effective Bohr radius), where the reduced mass μ is

$$1/\mu = 1/m_{oe} + 1/m_{oh} \tag{6}$$

and m_{oe} (m_{oh}) is the optical masses of the electron (the hole) defined as

$$1/m_{oe} = \tfrac{1}{3}(1/m_{\parallel e} + 2/m_{\perp e}), \tag{7a}$$

$$1/m_{oh} = \tfrac{1}{3}(1/m_{\parallel h} + 2/m_{\perp h}). \tag{7b}$$

The density-of-states masses are given by

$$m_{de} = (m_{\parallel e} m_{\perp e}^2)^{1/3}, \tag{8a}$$

$$m_{dh} = (m_{\parallel h} m_{\perp h}^2)^{1/3}. \tag{8b}$$

The dimensionless parameter r_s is defined as

$$r_s = (3/4\pi n)^{1/3}(1/a_x). \tag{9}$$

The function $\phi(\rho)$ is given by

$$\phi(\rho) = \rho^{1/6}\left(\frac{\sin^{-1}[(1-\rho)^{1/2}]}{(1-\rho)^{1/2}}\,\Theta(1-\rho) + \frac{\sinh^{-1}[(\rho-1)^{1/2}]}{(\rho-1)^{1/2}}\,\Theta(\rho-1)\right), \tag{10}$$

with

$$\rho = m_\perp / m_\parallel \tag{11}$$

and $\Theta(\rho) = 1$ for $0 \leqslant \rho \leqslant 1$ and zero otherwise.

For the case of two coupled valence bands the hole contribution to the Hartree-Fock energy in the spherical approximation is given by

$$E_{\mathrm{HF}}^{\mathrm{cv}} = E_K^{\mathrm{cv}} + E_{\mathrm{ex}}^{\mathrm{cv}}, \tag{12}$$

$$E_K^{\mathrm{cv}} = (2.2099/r_s^2)[\mu/m_H(1+\gamma^{3/2})^{2/3}]E_R, \tag{13}$$

$$E_{\mathrm{ex}}^{\mathrm{cv}} = -(0.9163/r_s)\psi(\gamma)E_R, \tag{14}$$

with

$$\psi(\gamma) = \frac{1}{4(1+\gamma^{3/2})^{4/3}}\left[-\tfrac{3}{4}(1-\gamma)^2 \ln\left(\frac{1+\sqrt{\gamma}}{1+\sqrt{\gamma}}\right) + 1 + \gamma^2 + 3\gamma^{3/2} + 3\gamma^{1/2} + \tfrac{3}{4}(1-\gamma^2)\int_{\sqrt{\gamma}}^{1}\frac{dx}{x}\ln\left(\frac{1+x}{1-x}\right)\right], \tag{15}$$

where

$$\gamma = m_L/m_H \tag{16}$$

(m_L is the light-hole effective mass; m_H is the heavy-hole effective mass).

The HF energy as given by the previous equations is accurate to within a few percent corrections due to warping. All the approximations, both in the nonpolar and in the polar case are contained in the correlation energy. In this paper, as in Brinkman and Rice,[14] we use the Hubbard approximation to calculate the correlation energy of the e-h liquid. This scheme of approximation agrees reasonably well both with the Combescot-Nozières (CN) approach[13] and the more sophisticated Vashishta, Das, and Singwi (VDS) scheme.[15] The chief advantage of the Hubbard approximation is its relative simplicity which leads to the possibility of including in the scheme the modifications due to the phonon coupling.

The coupling to LO phonons is included by adding to the Hamiltonian a term of the form

$$H = \sum_{\vec{p},\vec{k}\sigma} M(k)(a_{\vec{k}} + a_{-\vec{k}}^\dagger)(c_{\vec{p}+\vec{k}\sigma}^\dagger c_{\vec{p}\sigma} + b_{\vec{p}+\vec{k}\sigma}^\dagger b_{\vec{p}\sigma}), \tag{17}$$

where

$$M(k) = \{(2\pi e^2/k^2)[(\epsilon_0 - \epsilon_\infty)/\epsilon_\infty\epsilon_0]\,\omega_L\}^{1/2}. \tag{18}$$

and $a_{\vec{k}}^\dagger\,(a_{\vec{k}})$, $c_{\vec{k}}^\dagger(c_{\vec{k}})$, $b_{\vec{k}}^\dagger\,(b_{\vec{k}})$ are creation (destruction) operators for LO phonons, electrons, and holes, respectively, while ϵ_0 and ω_L are the static dielectric constant and the LO phonon frequency. Within the RPA, inclusion of the LO coupling leads to the diagrammatic expansion indicated in Fig. 1 where interaction lines correspond to the Coulomb interaction

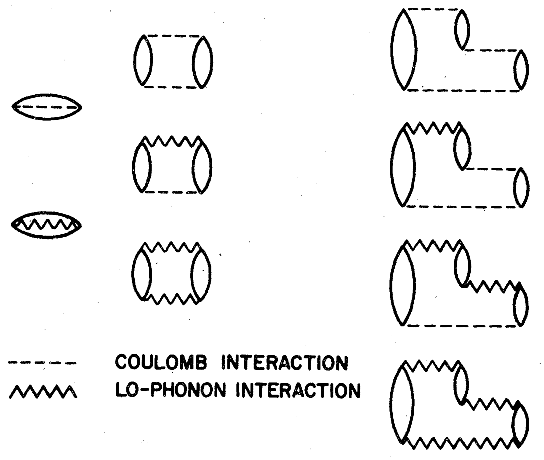

FIG. 1. First-, second-, and third-order diagrams for the RPA including LO-phonon coupling. The Coulomb interaction is Eq. (19) and the effective, LO-phonon mediated, interaction is Eq. (20).

$$V(k) = 4\pi e^2/k^2\epsilon_\infty, \tag{19}$$

and the effective (phonon-mediated) interaction

$$V_{ep}(k) = V(k)(\omega_T^2 - \omega_L^2)/(\omega_L^2 - \omega^2 - i\delta), \tag{20}$$

and ω_T is the transverse phonon frequency. Thus, in the RPA, the correlation energy per pair is

$$E_c = -\frac{1}{n}\int\frac{d^3k}{(2\pi)^3}\int_0^\infty\frac{d\omega}{2\pi} \times \int_0^1\frac{d\lambda}{\lambda}\,\mathrm{Im}\left(\frac{\lambda\tilde{V}\pi}{1-\lambda\tilde{V}\pi} - \lambda V\pi\right), \tag{21}$$

where

$$\tilde{V} = V + V_{ep} \tag{22}$$

and $\pi = \pi(\vec{k}, \omega)$ is the polarization part which we discuss below. This expression was used by Keldysh and Silin[5] as a starting point for their density expansions. We make the plausible assumption that the Hubbard method of including (approximately) the diagrams exchange-conjugates to the RPA diagrams, can be carried over to the phonon-coupled case. That is to say, we replace the polarizability $\lambda\tilde{V}\pi$ by

$$\lambda\tilde{V}\pi \to \lambda\tilde{V}\pi/[1 + f(k)\lambda\tilde{V}\pi], \tag{23}$$

where $f(k) = 0.5k^2/(k^2 + k_F^2)$ for a one-component system. The generalization to a multicomponent system with different masses is straightforward and a useful approximation has been discussed in Eq. (2.9) of Ref. 14. For the purpose of numerical calculation it is very convenient to distort the ω contour to go along the imaginary ω axis. (This gives a real integrand and it is not necessary to take into account explicitly the collective modes.) Thus, for ν_e (ν_h) valleys in the conduction (valence) band, we obtain

$$E_c = \frac{1}{n} \int \frac{d^3k}{(2\pi)^3} \int_0^\infty \frac{d\omega}{2\pi} [1 - f(k)(\nu_e + \nu_h)^{-1}]^{-1} \times (\ln\{1 - [1 - f(k)(\nu_e + \nu_h)^{-1}] \times \tilde{V}(\vec{k}, i\omega)\pi(\vec{k}, i\omega)\} + V(k)\pi(\vec{k}, i\omega)), \tag{24}$$

where

$$\pi(\vec{k}, i\omega) = \sum_{i=1}^{\nu_e+\nu_h} \pi_i(\vec{k}, i\omega) \tag{25}$$

and $\pi_i(\vec{k}, i\omega)$ is the ith valley polarization part given by

$$\pi_i(\vec{k}, i\omega) = 2 \sum_{\vec{p}\sigma} n_{p\sigma}^{(i)} \frac{\epsilon_{\vec{p}}^{(i)} - \epsilon_{\vec{p}+\vec{k}}^{(i)}}{(\epsilon_{\vec{p}}^{(i)} - \epsilon_{\vec{p}+\vec{k}}^{(i)})^2 + \omega^2}, \tag{26}$$

with

$$n_{p\sigma}^{(i)} = \Theta(\epsilon_{p_F}^{(i)} - \epsilon_p^{(i)}), \tag{27}$$

$$\epsilon_p^{(i)} = p_\parallel^2/2m_\parallel^{(i)} + p_\perp^2/m_\perp^{(i)}, \tag{28}$$

$$p_F^{(i)} = (3\pi^2 n^{(i)})^{1/3}. \tag{29}$$

With obvious notation, $n^{(i)}$, $m_\parallel^{(i)}$, and $m_\perp^{(i)}$ are, respectively, the ith valley carrier density, longitudinal, and transverse band masses.

Thus, for an isotropic valley we obtain

$$\pi_i(\vec{k}, i\omega) = \frac{p_F^{(i)} m^{(i)}}{2\pi^2} \left[-1 + \frac{1}{2\tilde{k}} \left(1 + \frac{\tilde{\omega}^2}{\tilde{k}^2} - \frac{\tilde{k}^2}{4}\right) \ln \left| \frac{(1 - \frac{1}{2}\tilde{k})^2 + (\tilde{\omega}/\tilde{k})^2}{(1 + \frac{1}{2}\tilde{k})^2 + (\tilde{\omega}/\tilde{k})^2} \right| + \frac{\tilde{\omega}}{\tilde{k}} \left(\tan^{-1} \frac{\tilde{k}(1 + \frac{1}{2}\tilde{k})}{\tilde{\omega}} + \tan^{-1} \frac{\tilde{k}(1 - \frac{1}{2}\tilde{k})}{\tilde{\omega}} \right) \right], \tag{30}$$

where

$$\tilde{k} \equiv k/p_F^{(i)}, \tag{31}$$

$$\tilde{\omega} = \omega/(2\epsilon_{p_F^{(i)}}^{(i)}). \tag{32}$$

The anisotropic valley polarizability $\pi_{iA}(\vec{k}, i\omega)$ is obtained from the scaling relationship

$$\pi_{iA}(\vec{k}, i\omega) = \pi_i(\vec{k}', i\omega, m_d), \tag{33}$$

where the right-hand side denotes $\pi_i(\vec{k}', i\omega)$ with $m^{(i)}$ replaced everywhere by the density-of-states mass $m_d = (m_\parallel m_\perp^2)^{1/3}$; k' is related to k by the transformation

$$k_\perp' = k_\perp \rho^{-1/6}, \tag{34a}$$

$$k_\parallel' = k_\parallel \rho^{1/3}. \tag{34b}$$

The case of two coupled valence bands is more complicated. A considerable simplification is obtained by introducing the isotropic approximation of Luttinger[16] used also by Combescot and Nozières[13] in their calculation of the ground-state energy. They showed that the effect of the coupling could be represented by introducing the matrix element

$$\Lambda(\vec{k}, \vec{k}') = \tfrac{1}{4}[1 + 3(\vec{k} \cdot \vec{k}'/kk')^2] \tag{35}$$

for coupling between like bands. Unlike bands are coupled by $1 - \Lambda(\vec{k}, \vec{k}')$. Therefore, the total polarization part for the two bands may be written as the sum of the contributions of the two noninteracting bands plus the coupling term $\Delta\pi$ given by

$$\Delta\pi_{ij} = 2 \sum_{\sigma\vec{p}} [1 - \Lambda(\vec{p}, \vec{p} + \vec{k})] \left[n_{p\sigma}^{(i)} \left(- \frac{\epsilon_p^{(i)} - \epsilon_{\vec{p}+\vec{k}}^{(i)}}{(\epsilon_p^{(i)} - \epsilon_{\vec{p}+\vec{k}}^{(i)})^2 + \omega^2} + \frac{\epsilon_p^{(i)} - \epsilon_{\vec{p}+\vec{k}}^{(j)}}{(\epsilon_p^{(i)} - \epsilon_{\vec{p}+\vec{k}}^{(j)})^2 + \omega^2} \right) + n_{p\sigma}^{(j)} \left(- \frac{\epsilon_p^{(j)} - \epsilon_{\vec{p}+\vec{k}}^{(j)}}{(\epsilon_p^{(j)} - \epsilon_{\vec{p}+\vec{k}}^{(j)})^2 + \omega^2} + \frac{\epsilon_p^{(j)} - \epsilon_{\vec{p}+\vec{k}}^{(i)}}{(\epsilon_p^{(j)} - \epsilon_{\vec{p}+\vec{k}}^{(i)})^2 + \omega^2} \right) \right]. \tag{36}$$

After some simple algebra (see Appendix), we obtain

$$\Delta\pi_{ij}(\vec{k}, i\omega) = (3k_0/32\pi^2)(1/\bar{k}) [F(m^{(j)}, m^{(i)}) - F(m^{(i)}, m^{(i)}) + F(m^{(i)}, m^{(j)}) - F(m^{(j)}, m^{(j)})], \tag{37}$$

where

$$k_0 = [3\pi^2(n^{(i)} + n^{(j)})]^{1/3} \tag{38}$$

and

$$\bar{k} = k/k_0 \tag{39}$$

and

$$F(m^{(j)}, m^{(i)}) = m^{(j)} \left\{ \frac{8\bar{k}}{(1+B^{3/2})^{1/3}} - \int_0^{1/(1+B^{3/2})^{1/3}} \frac{dx}{x} \left[-4x^2 B\gamma \ln \left| \frac{x+\bar{k}}{x-\bar{k}} \right| \right. \right.$$
$$+ 2(\gamma - 1)\left(\tan^{-1} \frac{(\bar{k}+x)^2 - x^2 B}{A^{(j)}} + \tan^{-1} \frac{(\bar{k}-x)^2 + x^2 B}{A^{(j)}} \right)$$
$$\left. \left. + [x^2 B(1+\gamma) - 2(\bar{k}^2 + x^2)] \ln \left| \frac{[(x+\bar{k})^2 - Bx^2]^2 + (A^{(j)})^2}{[(x-\bar{k})^2 + Bx^2]^2 + (A^{(j)})^2} \right| \right] \right\}, \tag{40}$$

with

$$A^{(j)} \equiv 2m^{(j)}\omega/k_0^2, \quad B \equiv m^{(j)}/m^{(i)} \tag{41}$$

and

$$\gamma(x) \equiv (x^2 - \bar{k}^2)^2/[B^2 x^2 + (A^{(j)})^2]. \tag{42}$$

An interesting limiting case is the low-density limit, which is obtained from (40) for $r_s \to \infty$ and which corresponds to the results for the single polaron energy shift of Refs. 11 and 12.

Finally, Eqs. (30) and/or (35) are substituted in Eq. (24) to obtain the correlation energy numerically. The integrals are two or three dimensional and have been calculated with an accuracy of $\approx 2.5\%$. Adding the correlation energy to the HF energy obtained from (1) and (12), we obtain the ground-state energy of the e-h liquid. We remark that all the masses appearing in the formulas of this section are bare band masses (not polaron masses) since all polaron effects are included in the correlation energy, Eq. (24). In fact, the polaron problem is completely described by (24) in the lowest order in $V_{ep}\pi$ [and, of course, setting $f(k)$ equal to zero].

III. RESULTS

In Sec. II, we have derived expressions general enough to include all the band-structure cases which we shall present in this section. We divide the compounds into three groups; (A) CdS, CdSe, AgBr, ZnS, and ZnO which have simple band structures and for which there are experimental results (except for ZnS); (B) cubic crystals with a coupled valence-band structure: the elements Ge and Si, the II-VI compounds CdTe, ZnSe, ZnTe and the III-V compounds AlAs, GaP, GaSb, InP, InSb; and (C) thallous halides TlBr and TlCl and lead chalcogenides which are strongly polar and have multivalley band structures.

A. CdS, CdSe, ZnO, ZnS, and AgBr

These II-VI compounds have the hexagonal wurtzite structure.[17] In this structure the electron minimum is at the Γ point and in Table I we list the polaron masses obtained by a variety of optical and resonance experiments. The valence band is split into three doubly degenerate (including spins) subbands by the combination of crystal-field and spin-orbit coupling. The splitting between the upper subbands, referred to as A and B, is fairly large and also listed in Table I. If we ignore the B subband entirely then we find that in all cases except ZnO the hole Fermi energy is smaller than the subband splitting and our approximation of ignoring the B subband is reasonable. However, in ZnO the splitting[18] is the smallest (~5 meV) and the Fermi energy is the largest so that we take the opposite or cubic limit and ignore the A-B splitting. In this case the A and B subbands are degenerate even at finite $\vec{k}$. The spin-orbit effects are much less than crystal-field splittings in contrast to the zinc-blende structure discussed in Sec. III B. Because of this subband degeneracy, at finite $\vec{k}$, there is no need to explicitly consider interband coupling. We treat the hole bands in ZnO as fourfold degenerate (including spin). The polaron mass parameters for the holes are listed in Table I. Also listed there are the experimental values of the LO phonon energy (ω_L) and the static (ϵ_0) and high-frequency (ϵ_∞) dielectric constants. From these values we can define the dimensionless polar coupling constant

$$\alpha_0 = e^2(1/\epsilon_\infty - 1/\epsilon_0)(m/2\omega_L)^{1/2}, \tag{43}$$

where m is the free-electron mass. The individual polar coupling constants for electrons (α_e) and holes (α_h) are simply obtained by substituting the bare density-of-states mass ($m^d_{e,h}$) for m in Eq. (43). In these compounds the static dielectric constant ϵ_0 is anisotropic. For simplicity we have averaged the static dielectric constant as follows:

$$1/\epsilon_0 \equiv \tfrac{1}{3}(2/\epsilon_{0\perp} + 1/\epsilon_{0\parallel}), \tag{44}$$

where $\epsilon_{0\perp,\parallel}$ is the transverse (longitudinal) dielectric constant. Since the anisotropy is small, this averaging procedure does not introduce large errors. Similarly, we neglect the anisotropy of the LO-phonon modes.

TABLE I. List of parameters used in the calculations. E_X is the exciton binding energy, α_0 is the polaron coupling constant, and Δ is the splitting between the two highest valence bands. The bare masses (unstarred) are obtained from the polaron masses (starred) as indicated in the text.

	m_e^*	m_e	$m^*_{h\parallel}$	$m_{h\parallel}$	$m^*_{h\perp}$	$m_{h\perp}$	ϵ_0	ϵ_∞	ω_L (meV)	E_X (meV)	α_0	Δ (meV)
CdS	0.205^a	0.185	5.0^a	4.38	0.7^a	0.555	8.58^b	5.86^b	36.8^b	27^b	1.41	15.2^c
CdSe	0.13^d	0.116	2.5^d	2.25	0.45^d	0.38	9.4^b	6.2^b	26.1^b	15^d	1.25	26.4^c
ZnS	0.28^c	0.25	1.4^c	1.25	0.49^c	0.41	8.6^e	5.2^e	43.6^e	36^f	1.34	28.4^c
ZnO	0.28^g	0.24	2.27	1.9^h	0.79	0.6^h	8.59^j	4.0^j	72^k	59^i	1.84	4.9^i
AgBr	0.288	0.221^l	1.71	1.25^m	0.79	0.52^m	10.6^n	4.68^n	17.3^o	16^p	3.35	79.9^q

[a] J. J. Hopfield and D. G. Thomas, Phys. Rev. 122, 35(1961); J. J. Hopfield, J. Phys. Chem. Solids 18, 97(1960).

[b] D. L. Rode, in *Semiconductors and Semimetals* (Academic, New York, 1975), Vol. 10, p. 84.

[c] B. Segall and D. T. F. Marple, in *Physics and Chemistry of II-VI Compounds*, edited by M. Aven and J. S. Prener (North-Holland, Amsterdam, 1965).

[d] J. O. Dimmock and R. G. Wheeler, J. Appl. Phys. 32, 2271(1961); R. G. Wheeler and J. O. Dimmock, Phys. Rev. 125, 1805(1962).

[e] C. S. Arguello, D. L. Rousseau, and S. P. S. Porto, Phys. Rev. 181, 1351(1969).

[f] R. G. Wheeler and J. O. Miklazz, in *Proceedings of the Seventh International Conference on Physics of Semiconductors*, edited by M. Hulin (Dunod, Paris, 1967), p. 873.

[g] K. J. Button, D. R. Cohn, M. vonOrtenbert, B. Lax, E. Mollwo, and R. Helbig, Phys. Rev. Lett. 28, 1637(1972).

[h] J. Chelikowsky (private communication).

[i] K. Hummer, Phys. Status Solidi B 56, 249(1973).

[j] H. Jaffe and D. A. Berlincourt, Proc. IEEE 53, 1372(1965); ϵ_∞ from Lyddane-Sachs-Teller relationship.

[k] D. C. Reynolds, C. W. Litton, and T. C. Collins, Phys. Status Solidi 12, 3(1965).

[l] J. W. Hodby, J. C. Crowder, and C. C. Bradley, J. Phys. C 7, 3033(1974).

[m] H. Tamura and T. Masumi, Solid State Commun. 12, 1183(1973).

[n] R. P. Lowndes and D. H. Marton, Proc. R. Soc. Lond. A 308, 473(1969).

[o] R. P. Lowndes, Phys. Rev. B 6, 1490(1972).

[p] G. Ascarelli, Phys. Rev. 179, 797(1969).

[q] P. M. Scop, Phys. Rev. 133, A934 (1965).

The energy shift of the bottom of the band $-E_p$ is given by

$$-E_p = -[\alpha_e \phi(\rho_e) + \alpha_h \phi(\rho_h)]\omega_L , \tag{45}$$

where ρ is the mass ratio $m_\perp / m_\parallel$ and $\phi(\rho)$ is defined in Eq. (10).

We have taken into account the anisotropy of the effective masses by calculating the longitudinal ($m^*_{e,h\parallel}$) and transverse ($m^*_{e,h\perp}$) effective polaron masses in the intermediate coupling approximation[19]

$$m^*_{e,h\parallel,\perp} = m_{e,h\parallel,\perp}[1 + \tfrac{1}{6}\alpha_0 \psi_{\parallel,\perp}(\rho_{e,h})] , \tag{46}$$

where

$$\psi_\parallel(\rho) = (m_\parallel / m)^{1/2}[3\rho^{3/2}F(\rho)] , \tag{47}$$

$$\psi_\perp(\rho) = (m_\perp / m)^{1/2}\{\tfrac{3}{2}[\rho^{-1/2} - F(\rho)]\}, \tag{48}$$

and

$$F(\rho) = \Theta(1-\rho)\frac{1}{(1-\rho)^{3/2}}\left[\left(\frac{1-\rho}{\rho}\right)^{1/2} - \sin^{-1}(1-\rho)^{1/2}\right]$$
$$+\Theta(\rho-1)\frac{1}{(\rho-1)^{3/2}}$$
$$\times\left[-\left(\frac{\rho-1}{\rho}\right)^{1/2} + \sinh^{-1}(\rho-1)^{1/2}\right] . \tag{49}$$

We use Eq. (46) to determine the band effective masses ($m_{e,h}$), which we require as input for our calculations, from the experimentally measured polaron masses ($m^*_{e,h}$) and these are also given in Table I.

There are two other types of interaction between carriers which are neglected in our approach. One is the piezoelectric polar coupling. This has been considered for CdS by Mahan and Hopfield[20] who showed that it leads to important changes in the effective mass but only at very low energies (<1 meV). The energy scale in our calculations is much larger and we shall ignore this effect. The second interaction is the exchange splitting between the excitons with parallel (antiparallel) electron and hole spins. Hopfield and Thomas[21] determined a value of 2.1 meV for this splitting in CdS. Again it is a small correction and we shall neglect it. In ZnO the effect is biggest and by scaling the CdS results we estimate the splitting could be as large as ≈14 meV. In the *e-h* liquid phase if we assume no spin dependent correlations between electrons and holes we would crudely estimate a repulsive contribution to the electron-hole energy of one-half of this splitting or ≈7 meV in ZnO. A better estimate requires consideration of the enhanced density in the liquid relative to an exciton and the spin dependent correlations—effects which tend to cancel. For ZnO, the effect is only ≈3% of E_G and we neglect it. For the semiconductors discussed in later subsections, the exciton is more weakly bound and the spin exchange effects are much smaller.

The ground-state energy was calculated from (2), (3), and (24) using the band-structure parameters listed in Table I as input. In Fig. 2 the results are presented for the II-VI compounds and the numbers are given in Table II. The zero of energy is the bare band gap. On the sides of the figure, the position of the band gap including the polar shift determined by (45), is indicated by the upper arrow. The lower arrow denotes the position of the allowed free exciton energy (i.e., antiparallel electron and hole spins) and the separation of the two arrows is the experimental exciton binding energy (E_x). In I we reported results for CdS, CdSe, and ZnS based on the plasmon pole approximation. In these materials our present results are close to those reported in I. The main difference arises from a slight change in the values of the masses. Previously we did not remove the polaron mass enhancement from the experimental values of the mass. We also have included the anisotropy in the polaron band shift rather than using the optical mass as in I. When all of these effects are included the changes are ≤10% of the total ground-state energy.

Recently, Rösler and Zimmerman[7] (RZ) have reported calculations for CdS, CdSe, and ZnS based on very similar approximations. The main differences between the two calculations are the inclusion of the Hubbard exchange correction here and the method of calculating E_G. They calculate the chemical potential in the RPA rather than E_G directly. Our value of $|E_G|$ is slightly smaller than theirs if we use polaron masses as they did, and this we attribute to the Hubbard exchange correction. Our results using the bare band masses as input is ~10% smaller in $|E_G|$. The use of bare masses also reduces the calculated single polaron shift but the change here is smaller than in $|E_G|$. The result is a substantial reduction in the binding energy E_B relative to the exciton defined by $E_B = |E_G| - E_X - E_P$.

While the changes in E_G are small, the changes in density are larger. Both our calculations and the RPA calculations of RZ show a sizable increase in equilibrium density relative to the plasmon pole approximation. We have no simple explanation for this change.

Experimental values have been reported[4] for CdS and CdSe. The binding energy $E_B \sim 13$ meV in CdS and $E_B \simeq 0$ meV in CdSe. Our new theoretical values give only a small binding energy of ≈1 meV in CdS and none at all in CdSe. However, while the changes in the binding energy are large, the changes in the total ground-state energy are only ~10%. We note that in calculating E_B we are subtracting two large number, e.g., in CdS, $|E_G| \approx 100$ meV. In addition there are substantial uncertainties in many of the input parameters. For example $m_{h\parallel}$ in CdS and CdSe is quite uncertain and $m_{h\perp}$ has experimental errors ≈(10–20)%. These uncertainties are larger than the polar renormalization of the masses (≈10%) which are responsible for the differences in E_B (≈10 meV in CdS) between our results here and in I. Also it has to be borne in mind that our theory of the correlation energy is approximate and for example in simple band structures in nonpolar materials the theories of Vashishta *et al.*[15] (VBS) and Inoue and Hanamura[22] give increases of this order in the correlation energy over the RPA. In view of these uncertainties, the overall agreement on the values of E_G is satisfactory even though the discrepancies in E_B look large.

The value of the equilibrium density is a more serious problem. Both our present calculation and that of RZ give numbers which are larger than those in I. The increase arises from the use of the methods based on the RPA but our values are less than those of RZ since we have used bare band masses as input. Even so, our value ($n_0 = 3.9\times 10^{18}$ cm^{-3}) in CdS is substantially greater than the experimental values which are in the range $n_0 \sim (1-2)\times 10^{18}$ cm^{-3}. At present, we have no explanation for this discrepancy.

In the Zn compounds, we have new calculations for ZnS and also now for ZnO. The former case is quite similar to CdSe and CdS in the relative energetics and we expect a corresponding similarity in its properties. In ZnO the conduction band has a single spherical minimum at the Γ point and the electron polaron mass has been determined experimentally (see Table I). The valence band is doubly degenerate as discussed above and we use the same mass for both subbands as determined in a recent band-structure calculation by Chelikowsky.[23] Note that these hole masses are quite anisotropic ($m_\perp/m_\parallel \sim 3$) as expected for II-VI compounds. Recent magneto-optical experiments of Hummer[18] deduced isotropic masses of a comparable magnitude but a comparison with other II-VI compounds favors substantial anisotropy. Using these values we compute a large value of the single polaron shift $E_P = 186$ meV which is larger than the effective Rydberg $E_R = 158$ meV (see Table II), in contrast to the other II-VI compounds. We find that the *e-h* liquid in our calculations lies above the exciton by ≈20 meV and the equilibrium density is ≈2×10^{19} cm^{-3}. Recently, Skettrup[24] has mea-

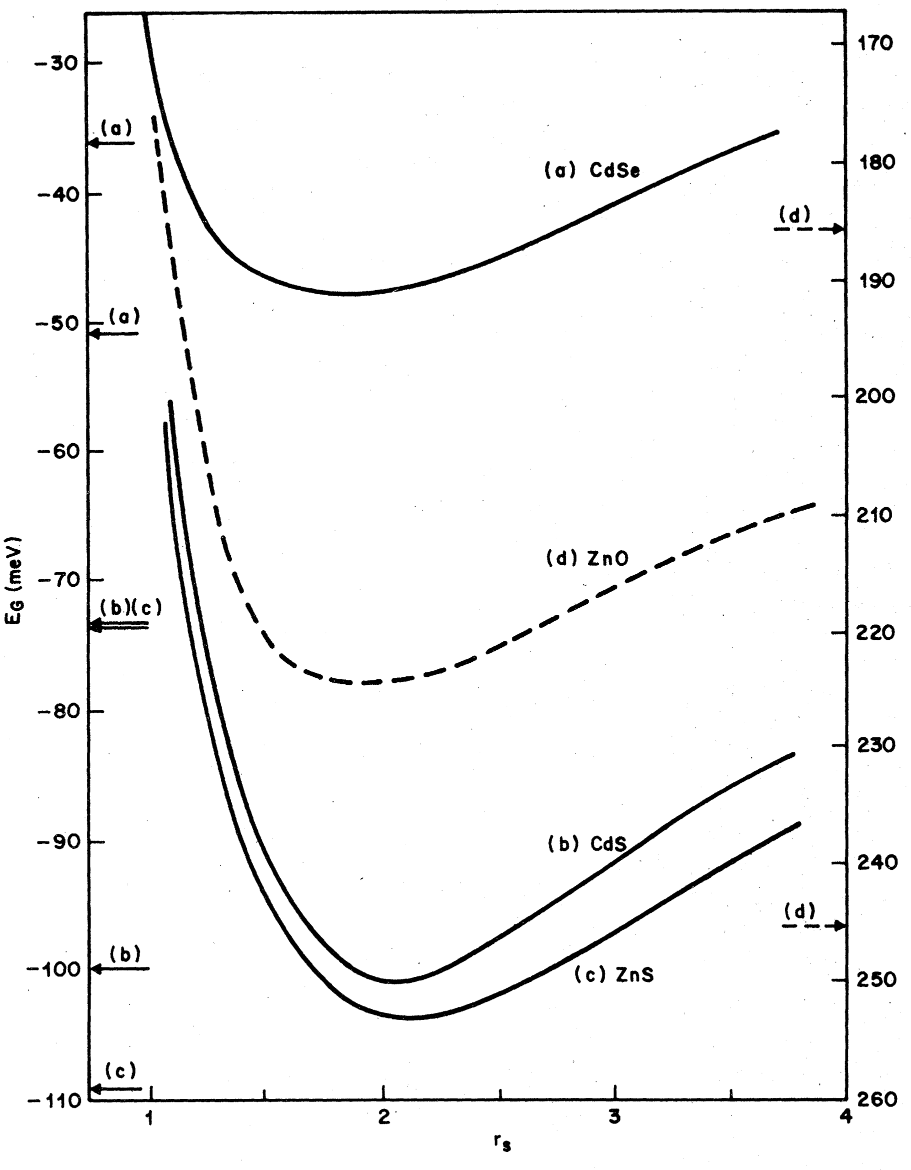

FIG. 2. Ground-state energy vs r_s for the e-h liquid including LO-phonon coupling for CdS, CdSe, ZnS (scale to the left), and ZnO (scale to the right). In each case the polaron ground-state energy is indicated by the upper arrow while the lower arrow indicates the experimental binding energy of the lowest exciton.

TABLE II. Calculated ground-state properties of the electron-hold liquid. E_R is the effective Rydberg [Eq. (5)]; E_P is the polaron shift [Eq. (45)]; $E_F^{e,h}$ are the electron (hole) Fermi energies; ω_p the plasma frequency; n_0 is the equilibrium density; E_G is the ground-state energy; and E_B is the binding energy of the liquid with respect to the free exciton, i.e., $E_B = |E_G| - E_X - E_P$.

	E_R (meV)	E_P (meV)	E_F^e (meV)	E_F^h (meV)	ω_p (meV)	n_0 (cm^{-3})	E_G (meV)	$\|E_G\| - E_P$ (meV)	E_B (meV)
CdS	73.7	73.1	50.7	7.7	84	3.9×10^{18}	−101.2	28.1	1
CdSe	33.6	36.7	21.0	3.4	35.5	5.4×10^{17}	−47.9	11.2	−4
ZnS	85.6	73.2	42.9	17.3	88	4.9×10^{18}	−103.9	30.7	−5
ZnO	158	186	116.3	19.9	201	2×10^{19}	−224.0	38	−21
AgBr	102.4	74.7	77.9	12.3	135	1.0×10^{19}	−121.0	46.3	+30

sured the optical gain in ZnO as a function of excitation intensity and temperature. The results are consistent with the observation of an *e*-*h* liquid with binding energy of ≈22 meV at a density of $\approx 1\times 10^{18}$ cm^{-3}. For ZnO the discrepancies between theory and experiment are larger than for the other II-VI compounds and the very large difference in densities makes it doubtful that Skettrup's experiments can be explained by an *e*-*h* liquid model, unless the values of the input parameters are seriously in error or some new effect outside our model is present.

Turning to AgBr, our new results are shown in Fig. 3. Compared to our results reported in I, there is a substantial increase in both $|E_G|$ and n_0. (Note that in the case of AgBr, the masses used in I were bare masses and there is no rescaling of the masses compared to the present calculation.) The change in ground-state properties reflects the considerable uncertainties introduced by the choice of the b coefficient in the plasmon dispersion in a multivalley band structure such as AgBr. The increase in density n_0 is similar to the change we found in the Cd compounds. Also, in Fig. 3 we show the results in two other approximations, the ϵ_0^* approximation and the complete neglect of polar coupling. In both approximations the only explicit interactions are the Coulomb interactions, screened by the static dielectric constant ϵ_0 and using polaron masses in the former case, while, in the latter, ϵ_∞ and bare band masses are used. Also, in the ϵ_0^* approximation the energy is referred to the band gap reduced by the polaron shift. We defer discussion of the comparison of the different approximations to Sec. III B.

Recently, Hulin *et al.*[3] have observed a new luminescence line in strongly pumped AgBr which has all the hallmarks of an *e*-*h* liquid line. By fitting the line shape they can obtain the binding energy E_B relative to exciton quite accurately and $E_B = 55$ meV in AgBr. To obtain a theoretical value of E_B we calculate E_P from Eq. (45) and use Ascarelli's experimental value[25] of $E_X = 16$ meV, giving us $E_B = 30$ meV. At this point, we note that the experimental value of E_X is surprisingly small.

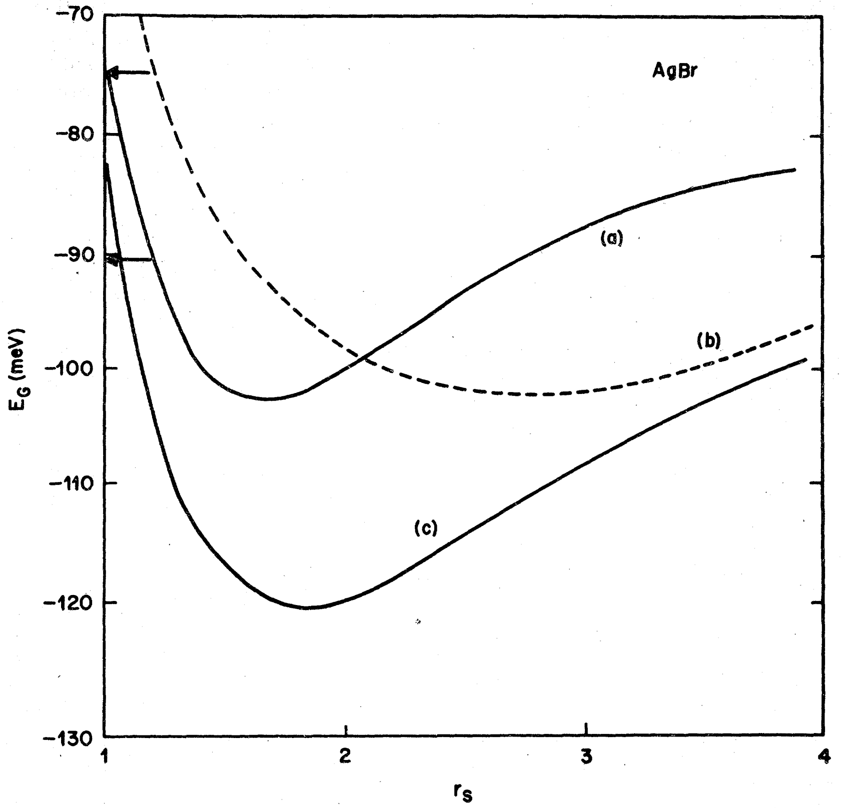

FIG. 3. Ground-state energy plotted against r_s for AgBr. Curve (a), pure Coulomb interaction (no phonons); curve (b), LO-phonon coupling included by replacing ϵ_∞ with ϵ_0, using the polaron effective masses and adding the polaron shift (ϵ_0^* approximation); curve (c), LO-phonon coupling included by the method described in the text. The arrows on the left indicate the polaron ground-state energy E_P (upper arrow) and the experimental binding energy of the lowest exciton (lower arrow).

It lies outside the range determined by E_R and $E_R(\epsilon_\infty/\epsilon_0)^2$, which is unusual. In addition, the excitonic molecule binding energy[26] E_M is ≈ 7 meV and the ratio $E_M/E_X \simeq \frac{7}{16}$ is much larger than expected on theoretical grounds.[27] Of course, any increase in E_X leads to a corresponding decrease in E_B from the value of 30 meV that we calculate and worsens the comparison to experiment. The luminescence line shape also gives an experimental value of $n_0 \approx 8\times 10^{18}$ cm^{-3} which agrees well with our theoretical number of $n_0 \approx 1\times 10^{19}$ cm^{-3}. One possible source of the discrepancy in E_B is the neglect of intervalley phonon scattering between the hole ellipsoids. In the absence of information on the relevant electron phonon matrix elements, we cannot estimate this correction to the effective-mass approximation.

B. Ge, Si and the cubic III-V and II-VI compounds

All of the materials in this subsection are cubic crystals and have a coupled valence-band structure.[17] Before discussing the polar effects, it is instructive to begin with the elemental semiconductors Ge and Si and we shall focus attention on the role of the valence-band coupling.

Several groups have calculated the correlation energy for Ge and Si.[1] The original Hubbard approximation calculation of Brinkman and Rice,[14] used four spherical electron bands and two spherical hole bands characterized by optical effective masses in the correlation energy. Combescot and Nozières[13] included the anisotropy of the electron bands and included valence band coupling in the spherical approximation discussed above. However, their method of calculating E_C based on the Nozières-Pines approximation involves a numerical interpolation and they estimate errors $\approx 10\%$ in their answers. Vashishta, Das, and Singwi[15] calculated the Hubbard approximation including anisotropy in the electrons but treated the hole bands in the decoupled optical mass approximation. They also included effects of the higher order electron-hole scattering, etc. Recently, Rose and Shore[28] made a complete RPA calculation for Ge including both anisotropy of the electrons and valence-band coupling in the spherical approximation. We have calculated E_C using the method described in Sec. II, namely, the Hubbard approximation with anisotropy of the electrons and valence band coupling in the spherical approximation. The results of all these groups are listed in Table III. Comparing first the Hubbard approximations, we see that our results are slightly below those of VDS,[15] and substantially below those of Brinkman and Rice.[14] From the earlier results of Vashishta, Bhattacharyya, and Singwi[15] we can estimate the affect of passing to the other limit of two uncoupled light and heavy mass valence bands. Our values in both Ge and Si lie close to halfway between such results and those of VDS.[15] Rose and Shore's results (RPA) for Ge lie very close to this limit and ≈ 0.5 meV below our results. While the Hubbard approximation should be slightly higher than the RPA, this discrepancy is rather more than expected. Our best results are obtained by adding the *e-h* scattering correction of VDS to the Hubbard approximation with all band structure effects included and are listed also in Table III. These values for both Ge and Si are in excellent agreement with the values quoted in the recent review of experiments by Hensel, Phillips, and Thomas.[1] This gives us confidence, in cases of multivalley band structure, in our procedures for estimating the ground-state energy without polar effects. Note that the electron-hole scattering correction in Ge

TABLE III. Experimental and theoretical ground-state energies (in meV) of *e-h* liquid in Ge and Si. Input parameters of our calculation are the same as in Ref. 14. HA means Hubbard approximation including anisotropy. FSC means fully self-consistent. δ is the estimated error due only to numerical computation.

	BR[a]	CN[b]	VDS[c]		RS[d]		This work		Experiment[e]
			HA	FSC	RPA	FSC	HA	FSC	
Ge	5.3	6.1 (5.8)[f]	5.8	5.9	6.57	6.65	6.1	6.2	6.0±0.2
Si	20.3	21.0	20.8	22.0			21.7	22.9	22.9±0.5
δ		10%	0.25%		5%[g]		2.5%		

[a] Reference 14.

[b] Reference 13.

[c] Reference 15.

[d] Reference 28.

[e] Reference 1.

[f] M. Combescot, Ph. D. thesis (University of Paris, 1973) (unpublished).

[g] J. H. Rose (private communication).

TABLE IV. Calculated ground-state properties of the EHL. E_R is the effective Rydberg [Eq. (5)]; E_P is the polaron shift [Eq. (45)]; $E_F^{e,h}$ are the electron (hole) Fermi energies; ω_p is the plasma frequency; n_0 is the equilibrium density; E_G is the ground-state energy; and E_B is the binding energy of the liquid with respect to the free exiton, i.e., $E_B = |E_G| - E_X - E_P$. Values given in parenthesis for GaAs, GaSb, InSb, and InP are obtained by using the ϵ_0^* approximation (with E_R in the appropriate units).

	E_R (meV)	E_P (meV)	E_F^e (meV)	E_F^h (meV)	ω_p (meV)	n_0 (cm^{-3})	E_G (meV)	$\|E_G\|-E_P$ (meV)	E_B (meV)
GaP	23.1	18.92	13.45	25.85	87.8	7.1×10^{18}	−48.8	29.9	11.9
AlAs	26.9	26.48	19.31	28.0	119.0	1.25×10^{19}	−59.0	32.45	14.5
CdTe	15.7	22.7	15.6	2.0	29.6	2.4×10^{17}	−32.7	10.0	0
ZnSe	32.9	32.6	46.0	7.8	86.7	3.2×10^{18}	−58.8	26.2	5
ZnTe	23.5	20.5	17.2	4.2	36.7	6.6×10^{17}	−34.8	14.3	3
GaAs	5.5	7.7	6.1	0.8	10.4	3.7×10^{16}	−10.0	2.7	
	(4.0)		(4.6)	(0.5)	(7.7)	$(2.4) \times 10^{16}$		(4.48)	(0.28)
GaSb	2.2	2.0	2.35	0.32	4.4	4.9×10^{15}	−2.3	0.3	
	(1.93)		(1.98)	(0.3)	(3.6)	$(4.0) \times 10^{15}$		(2.85)	(0.0)
InSb	0.5	2.1	0.65	0.02	1.0	1.1×10^{14}	−2.1	0.0	
	(0.4)		(0.46)	(0.01)	(0.8)	$(0.7) \times 10^{14}$		(0.6)	
InP	8.1	15.5	7.6	1.0	13.2	6.7×10^{16}	−15.6	0.1	
	(4.9)		(4.7)	(0.6)	(8.0)	$(3.3) \times 10^{16}$		(5.0)	(1.0)

and Si is not large and the band-structure effects we have included here is more important. However, for simpler bands the electron-hole scattering gives a larger effect.

Next we discuss the case of indirect gap polar materials GaP and AlAs. These materials are much less polar than those discussed above in Sec. III A and their band structures[17] have similarities to Ge and Si. We recently reported[9] our calculations in detail for GaP and here we merely quote the results in Table IV for completeness. Our results are in good agreement with the recent experiments of several groups.[2] AlAs is very similar to GaP in all properties but the uncertainties in the band parameters are larger.[29] In particular, it is not clear whether the conduction minimum is at the X point as calculated by Stukel and Euwema[30] or away from it at $(2\pi/a)(0.9, 0, 0)$ as calculated by Hess *et al.*[29] We shall assume the former but if the latter result is correct the *e-h* liquid will be more strongly bound. In the absence of detailed experimental results we use the theoretical estimates of the masses from Lawaetz,[31] Stukel and Euwema,[30] and Hess *et al.*,[29] quoted in Table V, as input. In both materials the *e-h* liquid is strongly bound. In GaP experiments give values for E_B and n_0 close to our calculation (see Table IV). No experiments have been reported to our knowledge in AlAs.

The direct-gap cubic III-V and II-VI semiconductors have a single spherical conduction band, coupled valence bands, and relative weak polar coupling especially for the III-V compounds. Considering first the II-VI compounds CdTe, ZnSe, and ZnTe there is a similarity to the hexagonal II-VI materials discussed in Sec. III A. The extra degeneracy arising from the coupling valence-band structure favors the *e-h* liquid. In Table VI we list the band parameters. In some cases they are accurately known from cyclotron resonance but in other cases we have used the values calculated by Lawaetz.[31] The polar correction to the masses for the coupled valence bands is taken from our previous work[12] and that of Trebin and Rossler.[11] If we compare to the hexagonal II-VI compounds, we see (Fig. 4 and Table IV) a distinct trend towards a larger binding for the *e-h* liquid which we believe is due to the degeneracy of the valence bands. These materials should be favorable cases to observe the *e-h* liquid but we know of no experiments at the present time. The case of CdTe has also been considered by RZ.[7] They, however, did not consider valence-band coupling and did not include the Hubbard exchange corrections effects which compensate so that our results and theirs are in close agreement.

In the cubic III-V compounds, there is a considerable amount of information on the band masses from cyclotron resonance and we have used these values where possible. In the case of GaAs, the complete calculation described above leads to a ground-state energy for the *e-h* liquid $|E_G| - E_P = 2.7$ meV which is 1.5 meV *above* the exciton. What is even more disturbing is that the ground state calculated in the ϵ_0^* approximation lies *below* the complete calculation (see Table IV). In fact the ϵ_0^* approximation including valence-band coupling, as discussed above, gives $|E_G| - E_P = 4.48$ meV leading to a small binding energy. The first calculation for GaAs in the ϵ_0^* approximation using optical mass averages, was that of Brinkman and

TABLE V. Indirect gap materials. List of parameters used in the calculation E_X is the free-exciton binding energy and α_0 is the polar coupling constant. Polaron masses are starred.

	$m_{e\parallel}^*$	$m_{e\parallel}$	$m_{e\perp}^*$	$m_{e\perp}$	m_{lh}^*	m_{lh}	m_{hh}^*	m_{hh}	ϵ_0	ϵ_∞	ω_L (meV)	α_0	E_X (meV)
Ge[a]		1.58		0.082		0.042		0.347	15.36				4.15
Si[b]		0.9163		0.1905		0.154		0.523	11.4				14.7
GaP[c]	2.032	1.781	0.254	0.25	0.163	0.15	0.479	0.46	11.02	9.07	50	0.322	18
AlAs	2.37	2.0[d]	0.245	0.24[e]	0.16	0.153[f]	0.67	0.652[f]	10.9[g]	8.5[g]	49.8[g]	0.428	18 ± 10[h]

[a] Reference 14.
[b] Reference 1.
[c] Reference 9.
[d] Reference 29.
[e] Reference 30.
[f] Reference 31.
[g] M. Ilegems and G. L. Pearson, Phys. Rev. B 1, 1576 (1970).
[h] M. R. Lorenz, R. Chicotka, G. C. Pettit, and P. J. Dean, Solid State Commun. 8, 693 (1970).

Rice[14] who obtained a value of $|E_G| - E_P = 3.7$ meV. Subsequently, VDS[15] used their electron-hole scattering method and obtained $|E_G| - E_P = 4.08$ meV. (Note both these calculations used an earlier value of ϵ_0 which was 4% larger.) Therefore, we can estimate 0.41 meV as the *e-h* scattering correction leading to a best value in the ϵ_0^* approximation of $|E_G| - E_P = 4.9$ meV which gives a value of $E_B = 0.7$ meV.

Shah *et al.*[32] have measured the absorption spec-

TABLE VI. Direct gap materials. List of parameters used in the calculation. E_X is the free-exciton binding energy and α_0 is the polar coupling constant. Polaron masses are starred.

	m_e^*	m_{lh}^*	m_{hh}^*	ϵ_0	ϵ_∞[a]	ω_L (meV)	α_0[b]	E_X (meV)
CdTe	0.0963[c]	0.103[d]	1.09[d]	10.31[e]	6.9	21.2[f]	1.21	10[g]
ZnSe	0.18[h]	0.149[d]	1.266[d]	8.8[e]	6.2	30.5[i]	0.99	21[j]
ZnTe	0.16[k]	0.15[l]	0.68[l]	9.9[m]	7.3	25.5[m]	0.83	11[n]
GaAs	0.0665[o]	0.085[o]	0.52[o]	12.35[e]	10.48	36.8[p]	0.278	4.2[q]
GaSb	0.047[r]	0.045[o]	0.32[o]	15.7[s]	14.4[s]	29.8[s]	0.118	2.8[t]
InSb	0.0134[c]	0.016[o]	0.39[o]	17.9[u]	15.7[v]	23.9[w]	0.185	
InP	0.0803[c]	0.12[o]	0.58[o]	12.6[u]	9.6[v]	42.8[x]	0.442	4.0[t]

[a] From LST relationship, if reference is not given.
[b] From Eq. (43).
[c] R. A. Stradling (private communication).
[d] Reference 31, polaron corrected as in Refs. 11 and 12.
[e] I. Strzalkowski, S. Joshi, and C. R. Cravell, Appl. Phys. Lett. 28, 350 (1976).
[f] J. Waldman, D. M. Larsen, P. E. Tarmenwald, C. C. Bradley, D. R. Cohn, and B. Lax, Phys. Rev. Lett. 23, 1033 (1969).
[g] C. Milloz and R. G. Wheeler, Phys. Rev. 153, 913 (1967).
[h] C. H. Henry, K. Nassau, and J. W. Schriever, Phys. Rev. B 5, 458 (1972).
[i] W. Taylor, Phys. Lett. A 24, 556 (1967).
[j] G. E. Hite, D. T. F. Maple, H. Aven, and B. Segall, Phys. Rev. 156, 850 (1967).
[k] D. L. Rode, Phys. Rev. B 2, 4036 (1970).
[l] R. A. Stradling, Solid State Commun. 6, 665 (1968).
[m] M. Balkaski, in *II-VI Semiconductor Compounds*, edited by D. G. Thomas (Benjamin, New York, 1967), p. 1007.
[n] R. E. Nahory and H. A. Fan, Phys. Rev. Lett. 17, 251 (1966).
[o] R. A. Stradling, College Int. Cent. Natl, Rech. Sci. 242, 317 (1975).
[p] A. L. Mears and R. A. Stradling, Solid State Commun. 7, 1267 (1969).
[q] D. D. Sell, S. E. Stokowski, R. Dingle, and J. V. Dilorenzo, Phys Rev. B 7, 4568 (1973).
[r] J. L. Robert and D. Barjow, C. R. Acad. Sci. (Paris) B 270, 350 (1970).
[s] M. Hass and B. W. Henvis, Phys. Chem. Solids 23, 1099 (1962).
[t] Reference 17.
[u] S. S. Mitra, J. Chem. Phys. 41, 3158 (1964).
[v] J. A. Van Vechten, Phys. Rev. 187, 1007 (1969).
[w] J. R. Apel and T. D. Poehler, Phys. Rev. B 4, 436 (1971).
[x] G. Lucowsky, R. M. Martin, and E. Burstein, Phys. Rev. B 4, 1367 (1971).

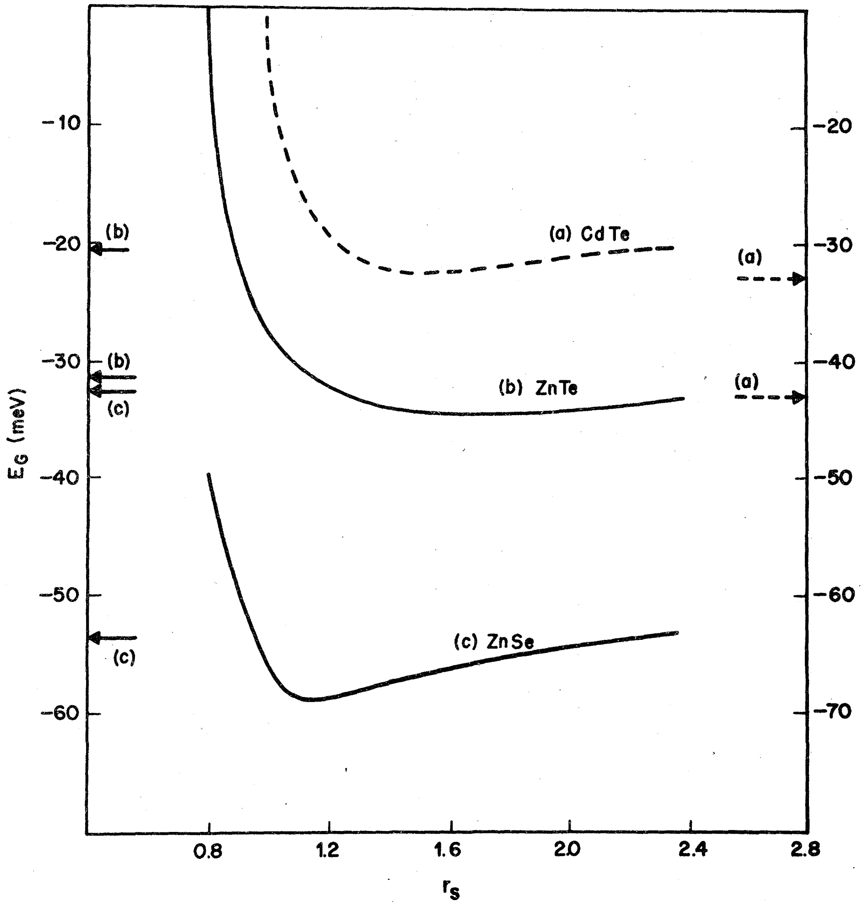

FIG. 4. Ground-state energy vs r_s for the *e-h* liquid including LO-phonon coupling for CdTe (scale to the right), ZnSe, and ZnTe (scale to the left). In each case, the polaron ground state energy is indicated by the upper arrow, while the lower arrow indicates the experimental binding energy of the lowest exciton.

tra of GaAs in the presence of intense optical pumping. They found that the exciton absorption broadens with increasing exciton intensity and that the threshold for the onset of absorption moves down below the band gap. The data can be fitted by including band gap renormalization and carrier heating. Their determination of the chemical potential relative to the polar shifted band gap ($\mu \equiv E_G + \partial E_G/\partial n + E_P$) $\mu \approx -9$ meV is consistent with the data of Hildebrand *et al.*,[33] who measured the gain spectra and found that the gain threshold lies ≈4 meV below the free exciton. They interpreted this result as evidence of *e-h* liquid phase with $E_B \approx 4$ meV, although carrier heating could also explain their result. More recently, however, Hildebrand and Göbel[34] reported transmission experiments at various photon energies of the exciting laser. In particular, by using an exciting energy identical to the exciton, heating is excluded and the carrier temperature can be estimated to be roughly the same as that of the sample. So, a strongly bound *e-h* liquid is suggested by these experiments. We have no explanation for the large discrepancy between the theoretical value of 0.7 meV and the value of ≈4 meV, especially since the uncertainties in the band parameters are less than in the case of strongly polar compounds.

Returning to the question of the difference between the results of the calculation based on the dynamic screening method of Sec. II and the ϵ_0^* approximation, we note first that in contrast with all polar materials discussed so far, we have here a case where $\omega_p \ll \omega_L$, or in other words we are at relatively low densities. In the low-density limit, Keldysh and Silin[5] concluded that the true ground-state energy would always lie below that calculated using a frequency-independent dielectric constant ϵ_0 and bare band masses. This was referred to in I as the ϵ_0 approximation. The ϵ_0^* approximation is the same except that the polaron mass correction is included. The Keldysh-Silin conclusion was based on the lowest order correction to the ϵ_0 approximation which is simply adding in the polaron mass correction. However, the answer we found in GaAs lies above not only the ϵ_0^* approximation but also the ϵ_0 approximation. The problem we believe arises from the use of the bubble sum, shown in Fig. 1, which neglects vertex and self-energy corrections. The initial dispersion of $\epsilon(\omega)$ in the *e-h* liquid is upward, leading to values *greater*

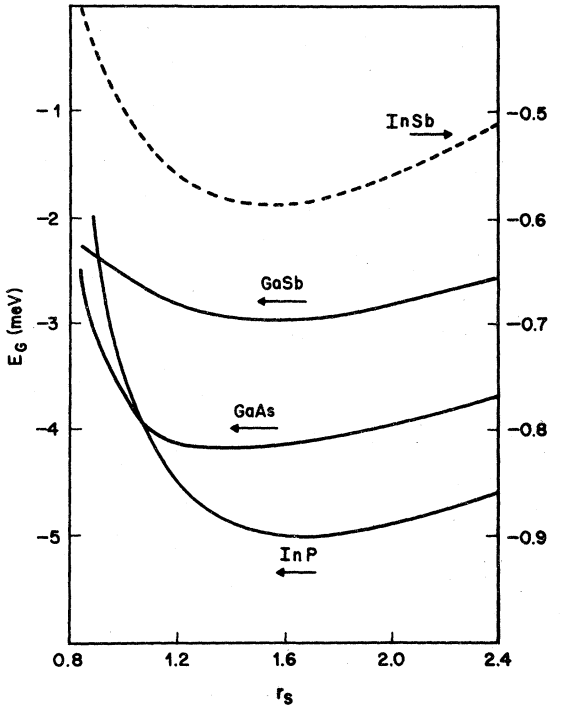

FIG. 5. Ground-state energy vs r_s for the e-h liquid in the ϵ_0^* approximation for InSb (scale to the right), GaSb, GaAs, and InP (scale to the left).

than ϵ_0. However, if one looks at the single electron-hole (i.e., exciton) problem, the effective Hamiltonian in this limit ($E_X/\omega_L \ll 1$) has been derived by Sak[35] and by Hattori.[36] These authors find that the two leading corrections to the ϵ_0^* approximation are a repulsive δ-function interaction between the electron and the hole and the velocity dependence of the polaron mass. These two effects cancel each other leading to a very small correction to E_X in GaAs, say. We believe that similar cancelling corrections will occur in the e-h liquid but a systematic expansion for the many electron-hole problem has not yet been carried out. For this reason, we conclude that the ϵ_0^* approximation is better than the dynamic screening method discussed above *in this limit*, $\omega_p \ll \omega_L$.

Turning to GaSb, InSb, and InP, we see from Table IV that in these cases the defects of the dynamic screening method are even more apparent. Again, we only get binding for the e-h liquid in the ϵ_0^* – approximation (see Fig. 5). For InP the situation is very similar to GaAs, discussed above. For GaSb and InSb, the scale of energies is very small and the equilibrium densities are very low. This will make it difficult to see an e-h liquid in equilibrium in these materials.

Lavallard *et al.*[37] have recently studied InSb at high density and observed an e-h fluid at densities $\sim 4 \times 10^{15}$ cm^{-3} more than an order of magnitude above n_0. However, for reasons that are unclear, they did not see the expected rapid expansion of this highly compressed fluid. We can obtain a value of the bottom of the band E_{BB} at this density from our results using the well known formula $E_{\mathrm{BB}}(n) = E_G(n) + n[\partial E_G(n)/\partial n]$. We obtain a value of $E_{BB} + E_P = -2.9$ meV at $n = 4.4 \times 10^{15}$ cm^{-3} which compares favorably with their experimental value of $E_{\mathrm{BB}} + E_P = -2.5$ meV.

C. TlBr, TlCl, PbS, PbSe, PbTe

It has been recently established that the thallous halides are indirect.[38] These materials have the CsCl structure. The single conduction-band minimum is at the R point and the valence band has three maxima located at the X points.[39] These ma-

TABLE VII. List of parameters used in the calculation. E_X is the free-exciton binding energy; α_0 is the polar coupling constant. For the thallous halides the bare masses are obtained from the polaron masses (starred) as indicated in the text.

	$m_{e\parallel}^*$	$m_{e\parallel}$	$m_{e\perp}^*$	$m_{e\perp}$	$m_{h\parallel}^*$	$m_{h\parallel}$	$m_{h\perp}^*$	$m_{h\perp}$	ϵ_0	ϵ_∞	ω_L	E_X	α_0
TlBr	0.52^{a}	0.35	0.52^{a}	0.35	0.55^{a}	0.386	0.74^{a}	0.491	35.1^{b}	5.41^{b}	14.3^{c}	23^{d}	4.82
TlCl	0.55^{a}	0.38	0.55^{a}	0.38	0.58^{a}	0.362	0.98^{a}	0.663	37.6^{b}	5.1^{b}	21.5^{c}	28.8^{e}	4.26
PbS	0.11^{f}		0.084^{f}		0.112^{f}		0.079^{f}		190^{g}	18.5^{h}	26.5^{g}		1.1
PbSe	0.052^{f}		0.035^{f}		0.068^{f}		0.034^{f}		280^{g}	25.2^{i}	18.2^{g}		0.99
PbTe	0.25^{f}		0.025^{f}		0.025^{f}		0.25^{f}		450^{g}	36.9^{i}	13.6^{g}		3.9

[a] Reference 40.
[b] R. Z. Bachrach and F. C. Brown, Phys. Rev. Lett. 19, 952 (1967).
[c] P. P. Lowdes and D. H. Martin, Proc. R. Soc. *A* 308, 473 (1969).
[d] Reference 41.
[e] Rescaled from E_X for TlBr (see text).
[f] *American Institute of Physics Handbook*, 3rd ed. (McGraw-Hill, New York, 1972).
[g] E. Burstein, S. Perkowitz, and M. H. Brodsky, J. Phys. Suppl. 11-12, C-4 (1968).
[h] F. C. Brown, in *Polarons and Excitons*, edited by C. G. Kuper and G. D. Whitfield (Plenum, London. 1962), p. 323.
[i] W. G. Spitzer, D. A. Kleinman, and C. J. Frosh, Phys. Rev. 113, 133 (1959).

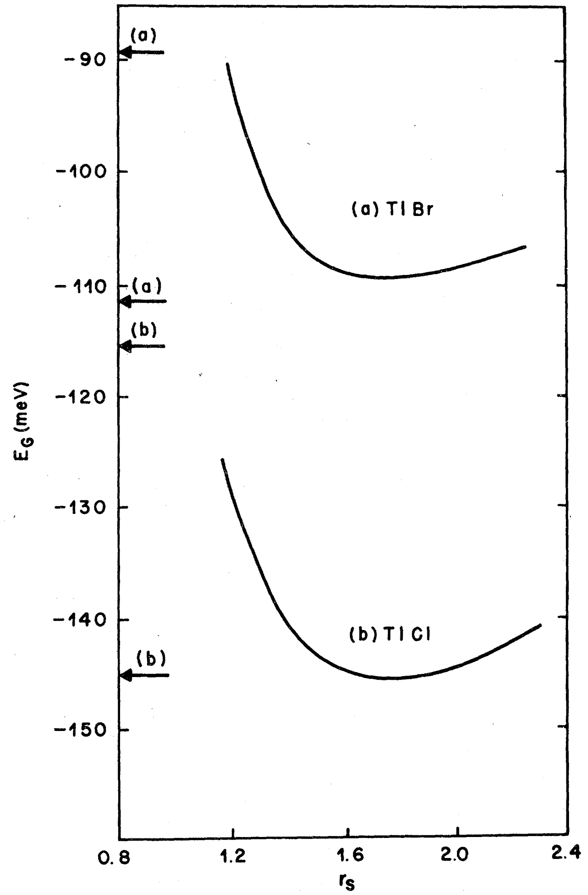

FIG. 6. Ground-state energy vs r_s for the *e*-*h* liquid including LO-phonon coupling for TlBr and TlCl. In each case the polaron ground-state energy is indicated by the upper arrow while the lower arrow indicates the experimental binding energy of the lowest exciton.

terials have quite large values of the polar coupling constants—comparable to AgBr. The effective masses have been measured by cyclotron resonance studies[40] and are listed in Table VII. It is interesting that the role of the anisotropy of the hole masses is reversed and $m_{h\parallel} < m_{h\perp}$. The exciton binding energy has been measured[41] by optical studies in TlBr. To obtain a value of E_X for TlCl we scale the value for TlBr by the ratios of E_R. The results are shown in Fig. 6 and Table VIII. We see that the values of $|E_G| - E_P$ are very close to E_X. The equilibrium densities are quite high, $n_0 \sim 10^{19}$ cm^{-3}. This suggests rapid Auger decay processes in the *e*-*h* liquid. However, by using techniques similar to those used by Hulin *et al.*,[3] it should be possible to observe an *e*-*h* liquid phase. It would be interesting to have experimental results for these cases to compare with AgBr. Also, it would be of interest to see if we underestimate E_B here as occurs in AgBr, CdS, and CdSe.

The lead chalcogenides form in the NaCl structure and are unusual in that they have a direct gap located at the L points of the Brillouin zone.[42] There is thus fourfold orbital degeneracy in both the electron and hole bands—a circumstance that clearly favors the *e*-*h* liquid. The masses have been determined by resonance techniques.[43] The exciton binding energies have not been measured to our knowledge. They have extremely large static dielectric constants. The value of ϵ_∞ is also large because of the small band gap. They therefore have very low values of the equilibrium density n_0 and are in the limit $\omega_p \ll \omega_L$ where our dynamic screening method is inapplicable. The results in the ϵ_0^* approximation are listed in Table VIII. While of some interest theoretically because they are large on the relative scale of E_R, on an absolute scale, the values of $|E_G| - E_P$ and n_0 are very small. This makes it very unlikely that pure enough materials and low enough carrier temperatures can be obtained to see an equilibrium *e*-*h* liquid in these materials.

IV. DISCUSSION AND CONCLUSIONS

The theory presented in the previous sections is an improvement over the plasmon pole approximation of I, and in view of the importance of the detailed nature of the band structures, we have taken care to include the coupling between the valence bands and also anisotropy where appropriate. Even so, there are still a number of serious limitations. One of the most important, is our imper-

TABLE VIII. Calculated ground-state properties of the EHL. E_R is the effective Rydberg [Eq. (5)]; E_P is the polaron shift [Eq. (4.5)]; $E_F^{e,h}$ are the electron (hole) Fermi energies; ω_p is the plasma frequency; n_0 is the equilibrium density; E_G is the ground-state energy; and E_B is the binding energy of the liquid with respect to the free exciton, i.e., $|E_G| - E_X - E_P$. Values for the lead chalcogenides are obtained using the ϵ_0^* approximation (with E_R in the appropriate units).

	E_R (meV)	E_P (meV)	E_F^e (meV)	E_F^h (meV)	ω_p (meV)	n_0 (cm^{-3})	E_G (meV)	$\|E_G\|-E_P$ (meV)	E_B (meV)
TlBr	91.5	89.0	61.9	23.0	137	1.4×10^{19}	109.8	20.8	−2.2
TlCl	114.5	115.8	75.2	25.3	164	2.2×10^{19}	144.7	28.9	0
PbS	0.017		0.012	0.012	0.06	2.4×10^{13}	0.025		
PbSe	0.0034		0.0029	0.0028	0.013	6.5×10^{11}	0.005		
PbTe	0.0012		0.0012	0.0012	0.007	2.9×10^{11}	0.0025		

fect knowledge of the input parameters, effective masses, dielectric constants exciton binding energies, etc. Since we end up comparing two large energies $|E_G|$ and E_P+E_X, small errors are greatly magnified in the comparison. For example, an error in the dielectric constants affects E_P and E_G in different ways. Even though we have taken the most accurate experimental values available, errors of the order of 10% in E_G are common.

A second serious limitation arises in the semiconductors where the *e-h* liquid occurs at low densities so that the carrier plasma frequency $\omega_p \ll \omega_L$. The III-V semiconductors GaAs, GaSb, InP, and InSb are examples of such materials. We commented briefly on this problem in Sec. III B. Let us compare the dynamic screening calculation to the ϵ_0^* approximation. The difference arises in the correlation energy [Eq. (21)]. By expanding the phonon factor at the relevant frequency ω_p,

$$\tilde{V}=V(\omega_p^2+\omega_T^2)/(\omega_p^2+\omega_L^2)$$
$$\simeq V(\omega_T^2/\omega_L^2)(1+\omega_p^2/\omega_T^2-\omega_p^2/\omega_L^2), \qquad (50)$$

in ω_p, it is easy to see that

$$(\tilde{V}\pi_{\epsilon_\infty})^2>(V\pi_{\epsilon_0^*})^2 \qquad (51)$$

where π_{ϵ_∞} (and $\pi_{\epsilon_0^*}$) are the polarization parts calculated with dynamic (and static) screening. Inequality (51) shows that the second order (in π) contribution to E_G is more negative in the ϵ_0^* approximation. As a result, if the equilibrium density is low enough that $\omega_p \ll \omega_L$, the ϵ_0^* approximation gives a lower E_G.

The trouble with the dynamic screening approximation is that, at low densities, we cannot retain only the diagrams indicated in Fig. 1 and neglect the vertex and self-energy corrections. As we pointed out in Sec. III, in this limit where the characteristic electronic energies are much smaller than ω_L and the polar coupling is weak, Sak[35] and Hattori[36] have derived an effective Hamiltonian for the single electron-hole (i.e., exciton) problem. The two leading corrections to the ϵ_0^* approximation are a repulsive δ-function interaction between the electron and hole and the velocity dependence of the polaron mass. These two effects tend to cancel leading to small net corrections. We conclude that in this limit, it is better to work with the ϵ_0^* approximation. This is in contrast to the conclusions of Keldysh and Silin[5] and of I. However, our calculations in I were limited to semiconductors for which $\omega_p \gg \omega_L$.

In fact, for most of the semiconductors, the limit $\omega_p \gg \omega_L$ applies and, in these cases, the dynamic screening method gives values of E_G below the ϵ_0^* approximation. An example is the case of AgBr where in Fig. 3 we show E_G as a function of r_s calculated in the ϵ_0^* approximation and by using the dynamic screening method. Also for comparison, we show the results of a calculation using only Coulomb interactions between the carriers screened by ϵ_∞. From these results, which are representative of the limit $\omega_p \gg \omega_L$, we see that the coupling to the optical modes stabilizes the *e-h* liquid.

It is reasonable to expect that the generalized RPA diagrammatic expansion (which as discussed in Sec. III B works well for $\omega_L=0$) will remain a good scheme of approximation for $\omega_p/\omega_L \gg 1$. Thus, it is somewhat surprising, but perfectly consistent, that in many cases, we can calculate more accurately the *e-h* liquid ground state energy than the exciton binding energy in a polar crystal. In fact, it occurs frequently, e.g., CdS, that $\omega_p \gg \omega_L$ while $E_X \lesssim \omega_L$. While a more general theory—to include cases for which $\omega_p \lesssim \omega_L$—will be considered in a future work, at this stage the criterion $\omega_p \gg \omega_L$ may be used *a posteriori* to assess the reliability of the calculation of the *e-h* liquid properties for a given semiconductor using the dynamic screening method.

For most of the materials that we have discussed, the values of $|E_G|$ and E_P+E_X are close. One exception where $\omega_P \gg \omega_L$ but *e-h* liquid ground state is found to be substantially higher than the free exciton is ZnO. One might have expected, because of the approximate degeneracy of the valence band, that the *e-h* liquid state would be favored. However, ZnO has a large value of the polaron shift of the band gap E_P. In fact, if we compare E_R (the characteristic interparticle Coulomb energy) to E_P, then ZnO is one of the few materials where $E_P > E_R$. Looking over our results, there appears a trend that the *e-h* liquid binding energy varies inversely with E_P/E_R. For example, in AgBr, this ratio is considerably less than one and E_B is large.

Another trend in our calculations appears to be a consistent underestimation of the value of E_B relative to experiment in the polar materials as exemplified by AgBr, CdS, and CdSe. The discrepancy is not very large (~10%) but in the nonpolar or weakly polar materials, e.g., Ge, Si, and GaP, the theory is very accurate. Perhaps, this arises from some deficiencies in our treatment of polar coupling or because of the relatively greater corrections due to electron-hole scattering in these materials with simpler band structures. The most puzzling discrepancy is between our theory and the experiments of Hildebrand and Gobel[34] in the case of GaAs. It is hard to see how any of the corrections discussed above can give a value of E_B as large as they have reported.

In this paper, we have restricted our calculations to zero-temperature properties. The formalism is easily applicable to finite temperature for the analysis of the thermodynamic properties of the *e-h* liquid. Reinecke[44] has calculated the phase diagram for CdS at finite temperatures in reasonable agreement with the experiments of Leheny and Shah.[4]

It is apparent from the calculation presented here, that formation of the *e-h* liquid is a widespread phenomenon. The observation in CdS and CdSe and recently in AgBr and GaP supports this conclusion. We hope that these calculations will lead to experiments on more semiconductors and enable us to test the trends that have emerged from our calculations.

Note added in proof. Since the preparation of the manuscript, new studies have been reported on (a) GaAs; (b) CdS, CdSe; and (c) SiC. (a) *GaAs*: A careful study of spontaneous luminescence by V. V. Stopachinskii [Sov. Phys. JETP 45, 310 (1977)] on ultrapure GaAs at low pump powers has led him to identify an *e-h* liquid line with $n_0 \approx 10^{16}$ cm^{-3} and $E_B \approx 1$ meV in very good agreement with our calculations. A series of luminescence, gain, transmission, and excitation spectra experiments by O. Hildebrand, E. O. Goebel, K. M. Romanek, H. Weber, and G. Mahler [Phys. Rev. B (to be published)] has led them to identify a luminescence line with a peak ≈5 meV lower as due to emission from an *e-h* plasma—an identification similar to that made in earlier work by T. Moriya and T. Kushida [J. Phys. Soc. Jpn. 43, 1646 (1977)]. Both of these studies are at high excitation power. Hildebrand *et al.* interpret their data in terms of a hot, dense, *e-h* plasma, but their analysis leads them to a value of the *e-h* pair energy some 5 meV below our calculation. In view of the agreement between theory and Stopachinskii's data at low powers on pure samples, the analysis of the high-power data needs to be reexamined. (b) *CdS and CdSe*: Recent time-resolved picosecond luminescence spectra [M. Hayashi, H. Saito, and S. Shionoya, Solid State Commun. 24, 833 (1977); *ibid.* 24, 837 (1977)] show a new luminescence line appears at very high excitation intensities in CdS and CdSe. The line becomes broader with increasing intensity and shifts to lower energy. Hayashi *et al.* attribute this line to a high-density *e-h* plasma. There is a strong similarity to the data at higher powers in GaAs discussed above. (c) *SiC*: Very recently D. Bimberg, M. S. Skolnick, and W. J. Choyke [Phys. Rev. Lett. 40, 56 (1978)] have reported the observation of an *e-h* liquid in cubic SiC. A straightforward application [G. Beni, T. M. Rice and L. A. Hemstreet (unpublished)] of a simple extension of the theory presented in this work gives results in excellent agreement with the experiments of Bimberg *et al.*

ACKNOWLEDGMENTS

We thank E. O. Kane, R. F. Leheny, and J. Shah for many useful discussions and we are grateful to J. Chelikowsky, R. Dingle, J. C. Hensel, W. D. Johnston, and R. A. Stradling for providing us with valuable information on the input parameters used in our calculations.

APPENDIX

To obtain Eq. (37) from Eq. (36) we write

$$\Delta\pi_{ij} = 2(I^{ij} - I^{ii} + I^{ji} - I^{jj}), \tag{A1}$$

where

$$I^{ij} \equiv \sum_{\substack{\sigma,\vec{p}\\ |p|<p'}} [1 - \Lambda(\vec{p}, \vec{p}+\vec{k})] \frac{\epsilon_p^{(i)} - \epsilon_{\vec{p}+\vec{k}}^{(j)}}{(\epsilon_p^{(i)} - \epsilon_{\vec{p}+\vec{k}}^{(j)})^2 + \omega^2}, \tag{A2}$$

with

$$p' \equiv p_F^{(i)}[B^{1/2} + \delta_{ij}(1 - B^{1/2})] \tag{A3}$$

and B given by Eq. (41). I^{ij} can be reduced to the following one-dimensional integral:

$$I^{ij} = \frac{2}{3\pi^2} m^{(j)} k^2 \int_0^{p'} dx\, x^2 (f_1 + f_2 f_3 + f_4 f_5), \tag{A4}$$

with

$$f_1 \equiv (1/4x^2k^3)\{2k - Bgx \ln[(x+k)/(x-k)]\}, \tag{A5}$$

$$f_2 \equiv [1/(2xk)^2]\{(x^2 - k^2)^2 - (2m^{(j)}\omega)^2 - x^4B^2g\}, \tag{A6}$$

$$f_3 \equiv \frac{1}{4xkm^{(j)}\omega}\left(\tan^{-1}\frac{2xk - [x^2(B-1)^2 - k^2]}{2m^{(j)}\omega} + \tan^{-1}\frac{2xk + [x^2(B-1)^2 - k^2]}{2m^{(j)}\omega}\right), \tag{A7}$$

$$f_4 \equiv [1/(2kx)^3]\{x^2(B-1) - k^2[1 + B(1-g)]\}, \tag{A8}$$

$$f_5 \equiv \ln\left(\frac{[2kx - x^2(B-1) + k^2]^2 + (2m^{(j)}\omega)^2}{[2kx + x^2(B-1) - k^2]^2 + (2m^{(j)}\omega)^2}\right), \tag{A9}$$

and

$$g \equiv (x^2 - k^2)^2[x^4B^2 + (2m^{(j)}\omega)^2]^{-1}. \tag{A10}$$

Finally, changing variables, one obtains Eq. (37) from (A4) and (A1).

[1] J. C. Hensel, T. G. Phillips, and G. A. Thomas in *Solid State Physics*, edited by F. Seitz, D. Turnbull, and H. Ehrenreich (Academic, New York, 1978), Vol. 32, p. 88; T. M. Rice, *ibid*., p. 1.

[2] J. Shah, R. F. Leheny, W. R. Harding, and D. R. Wight, Phys. Rev. Lett. 38, 1164 (1977); D. Hulin, M. Combescot, N. Bontemps, and A. Mysyrowicz, Phys. Lett. A 61, 349 (1977); H. Maaref, J. Barrau, M. Brousseau, J. Collet, and J. Mazzaschi, Solid State Commun. 22, 593 (1977).

[3] D. Hulin, A. Mysyrowicz, M. Combescot, I. Pelant, and C. Benoît à la Guillaume, Phys. Rev. Lett. 39, 1169 (1977).

[4] R. F. Leheny and J. Shah, Phys. Rev. Lett. 37, 871 (1976); 38, 511 (1977); V. G. Lysenko, V. I. Revenko, T. G. Tratas, and V. B. Timofeev, Sov. Phys.-JETP 41, 163 (1975).

[5] L. V. Keldysh and A. P. Silin, Zh. Eksp. Teor. Fiz. 69, 1053 (1975) [Sov. Phys.-JETP 42, 535 (1976)].

[6] G. Beni and T. M. Rice, Phys. Rev. Lett. 37, 874 (1976).

[7] M. Rösler and R. Zimmerman, Phys. Status Solidi B 83, 85 (1977).

[8] See, e.g., L. Hedin and S. Lundqvist, in *Solid State Physics*, edited by H. Ehrenreich (Academic, New York, 1969), Vol. 23, p. 32.

[9] G. Beni and T. M. Rice, Solid State Commun. 23, 871 (1977).

[10] See, e.g., *Polarons and Excitons*, edited by C. G. Kuper (Plenum, New York, 1963).

[11] H. R. Trebin and U. Rossler, Phys. Status Solidi B 70, 717 (1975).

[12] G. Beni and T. M. Rice, Phys. Rev. B 15, 840 (1977).

[13] M. Combescot and P. Nozières, J. Phys. C 5, 2369 (1972).

[14] W. F. Brinkman and T. M. Rice, Phys. Rev. B 7, 1508 (1973).

[15] P. Vashishta, P. Bhattacharyya, and K. S. Singwi, Phys. Rev. B 10, 5108 (1974) (VBS); P. Vashishta, S. G. Das, and K. S. Singwi, Phys. Rev. Lett. 33, 911 (1974) (VDS).

[16] J. M. Luttinger and W. Kohn, Phys. Rev. 97, 969 (1955).

[17] *Physics and Chemistry of II-VI Compounds*, edited by M. Aven and J. S. Prener (North-Holland, Amsterdam, 1965); *Semiconductors and Semimetals*, edited by R. K. Willardson and A. C. Beer (Academic, New York, 1967), Vol. 3.

[18] K. Hümmer, Phys. Status Solidi B 56, 249 (1973).

[19] M. Matsuura and S. Wang, Solid State Commun. 14, 533 (1974).

[20] G. D. Mahan and J. J. Hopfield, Phys. Rev. Lett. 12, 241 (1964).

[21] J. J. Hopfield and D. G. Thomas, Phys. Rev. 122, 35 (1961); 128, 2135 (1962).

[22] M. Inoue and E. Hanamura, J. Phys. Soc. Jpn. 35, 643 (1973).

[23] J. R. Chelikowsky, Solid State Commun. 22, 351 (1977).

[24] T. Skettrup, Solid State Commun. 23, 741 (1977).

[25] G. Ascarelli, Phys. Rev. 179, 797 (1969).

[26] I. Pelant, A. Mysyrowicz, and A. Benoît à la Guillame, Phys. Rev. Lett. 37, 1708 (1976).

[27] W. F. Brinkman, T. M. Rice, and B. Bell, Phys. Rev. B 8, 1570 (1973).

[28] J. H. Rose, and H. B. Shore, Phys. Rev. B 17, 1884 (1978).

[29] E. Hess, I. Topol, K. R. Schulze, H. Neumann, and K. Unger, Phys. Status Solidi B 55, 187 (1973).

[30] D. J. Stukel, and R. N. Euwema, Phys. Rev. 188, 1193 (1969).

[31] P. Lawaetz, Phys. Rev. B 4, 3460 (1971).

[32] J. Shah, R. F. Leheny, and W. Wiegmann, Phys. Rev. B 16, 1577 (1977).

[33] O. Hildebrand, B. O. Faltermeiner, and M. H. Pilkuhn, Solid State Commun. 19, 841 (1976).

[34] O. Hildebrand and E. Göbel, in *Proceedings of the Thirteenth International Conference on the Physics of Semiconductors*, edited by F. G. Fumi, (Marves, Rome, 1976); E. O. Göbel and O. Hildebrand Solid State Electron. (to be published).

[35] J. Sak, Phys. Rev. B 6, 2226 (1972).

[36] K. Hattori, J. Phys. Soc. Jpn. 38, 51 (1975).

[37] P. Lavallard, R. Bichard, and A. Benoît à la Guillaume, Phys. Rev. B 16, 2804 (1977).

[38] R. Shimizu, T. Koda, and T. Murahashi, J. Phys. Soc. Jpn. 36, 161 (1974).

[39] H. Overhof and J. Treusch, Solid State Commun. 9, 53 (1971).

[40] J. W. Hodby, G. T. Jenkin, K. K. Obayashi, and H. Tamura, Solid State Commun. 10, 1017 (1972).

[41] J. Nakahara, K. Kobayashi, and A. Fujii, J. Phys. Soc. Jpn. 37, 1312 (1974).

[42] Y. Ravich and B. A. Efimova, *Semiconducting Lead Chalcogenides* (Plenum, New York, 1970).

[43] E. D. Mitchell *et al*., *Proceedings of the Fourth International Conference on the Physics of Semiconductors*, edited by M. Hulin (Dunod, Paris, 1964), p. 325; K. P. Cuff *et al*., *ibid*., p. 677; S. Berman, Phys. Rev. 158, 723 (1967); H. Numata and Y. Yemara, J. Phys. Soc. Jpn. 19, 2140 (1964).

[44] T. L. Reinecke, Phys. Rev. B 16, 2653 (1977).